Intermittently coupled electricity markets

Erwan Pierre, Lorenz Schneider

Journal Pre-proof

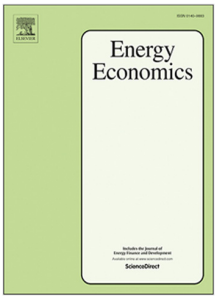

Intermittently coupled electricity markets

Erwan Pierre, Lorenz Schneider

PII: S0140-9883(24)00035-5
DOI: https://doi.org/10.1016/j.eneco.2024.107327
Reference: ENEECO 107327

To appear in: *Energy Economics*

Received date : 4 April 2023
Revised date : 23 November 2023
Accepted date : 10 January 2024

Please cite this article as: E. Pierre and L. Schneider, Intermittently coupled electricity markets. *Energy Economics* (2024), doi: https://doi.org/10.1016/j.eneco.2024.107327.

Intermittently Coupled Electricity Markets *

Erwan Pierre † Lorenz Schneider ‡

November 23, 2023

Abstract

Auctions of transmission rights between neighbouring countries are becoming increasingly active. In a parallel development, the introduction of market coupling frequently leads to smaller price differences between such countries. Indeed, if two countries are completely coupled, the price of a given hour of electricity will be identical in each country, resulting in a price spread of zero. Clearly, it is important to take this market coupling into account when evaluating transmission rights, as neglecting it would lead to a significant overvaluation of these rights. In order to address this issue, we introduce a general regime-switching mechanism that can be applied to many models in the literature. In particular, we focus on extending the model proposed by Cartea and González-Pedraz (2012). We describe the model estimation procedure in detail, and compare model and market prices of European spread options. We observe a dramatic paradigm shift in our data set at the end of the summer of 2021, and show that this shift has a strong effect on the model parameters. We also see that the reliable pricing and trading of spread options becomes problematic in such a volatile and uncertain market environment.

Keywords: Electricity Markets, Interconnectors, Market Coupling, Spread Options, Regime Switching

JEL: C51, C63, D44, G13, Q41

1 Introduction

European interconnected electricity markets

From the very beginning of its efforts to liberalise the European electricity markets in 1996, the European Commission has focused on ensuring the development of a secure and integrated market. In line with this objective, it set up an Expert Group to provide specific technical advice. The European Commission Expert Group (2017) states in its first report that "*Electricity interconnectors are the physical component of making this market truly European by connecting Member States' networks offering capacity for electricity trade, improved security of supply and allowing integration of the rapidly-growing share of renewable electricity production.*" The European Commission set the objective of increasing the electricity interconnection target to 15% by 2030, this ratio being defined as import capacity over installed generation capacity in a given Member State.

Since then, the European Commission Expert Group (2018) has made significant changes to this ratio to take into account the increasing share of renewables in the European energy mix. And in its

*We would like to thank Arthur Boidevézi, Rüdiger Kiesel, Jules Lafritte, Cassio Neri and Bertrand Tavin for their helpful comments and discussions.

†BCM Energy, erwan.pierre@elmy-energie.fr.

‡EMLYON Business School, schneider@em-lyon.com.

latest report, the European Commission Expert Group (2020) gave two main recommendations: "*First, interconnection targets must have a triple dimension, measuring: a) the degree of market integration, b) the capacity of interconnectors and related internal grid reinforcement for importing electricity, and c) the capacity of interconnectors and related internal grid reinforcement for exporting renewable electricity. Second, priority should be given to the more efficient functioning of the European electricity market.*" These broad guidelines for expanding the European grid are all the more important today, when tension in the grid is exacerbated by a geopolitical situation that is causing Member States to question sources of energy supply. Furthermore, since volatility and prices have increased substantially in recent months, the economic value of interconnections is all the greater, justifying significant investments.

The interconnection market is managed by the European Network of Transmission System Operators for Electricity (ENTSO-E), an association that, together with all European Transmission System Operators (TSOs), aims to fulfill the mission of: "*Ensuring the security of the interconnected power system in all time frames at pan-European level and the optimal functioning and development of the European interconnected electricity markets*". More concretely, this means that all market participants have access to an auction market to buy or sell transmission capacity rights in order to mitigate their risks. For each border and each horizon, an auction is held a few days before the timeframe delivery. From both a practical and a theoretical standpoint, this means that we need to consider the topic of option pricing.

Literature review

We now turn to a review of the literature on electricity markets, risk-neutral and real option pricing, interconnectors, and market-coupling. General introductions and overviews of real options are presented by Trigeorgis (1996) and Schwartz and Trigeorgis (2001). Clark (2014), Roncoroni et al. (2015) and Fanelli (2019) give general introductions to financial modelling in commodity markets. Burger et al. (2014) provide a comprehensive guide for risk management in energy markets.

Many authors model electricity prices using a fundamental, structural approach based on production inputs. Barlow (2002) develops a supply and demand model to obtain a diffusion model for electricity spot prices that can account for price spikes, which are an important empirical feature of electricity markets. Karakatsani and Bunn (2008) study regime-switching dynamics in intra-day electricity markets, and find that aggregate fundamental price models can help uncover important aspects of market performance, evolution and agent behaviour. Coulon and Howison (2009) model electricity prices within a fundamental bid stack framework that takes multiple fuel prices as input factors and addresses capacity or margin issues such as outages. A well-known drawback of the structural approach is that derivatives pricing can be slow and cumbersome. Füss et al. (2015) employ a fundamental approach, which nevertheless allows them to obtain tractable pricing methods, and then examine whether the inclusion of demand and capacity forecasts affects their model's pricing performance. Over the years, trading activity has increased in electricity markets, and this has led to a greater offer of tradeable products, such as new 15- and 30-minute contracts in addition to the traditional hourly ones. Following this development, Kiesel and Paraschiv (2017) perform an econometric analysis on a data set of 15-minute intra-day prices from the German market, and describe how these higher-frequency prices adjust to forecast errors.

Regarding option pricing, Carmona and Durrleman (2003) survey problems associated with the pricing and hedging of spread options. They focus on energy markets in particular, and on the numerical challenges encountered when working with various popular models. Kiesel et al. (2009) propose a two-factor model for electricity futures and calibrate it to option prices from the EEX. This model serves as a good example of the extent to which models can be simplified, compared to structural models, when the main goal is to perform forward and option pricing. This approach can still be significantly generalised, as shown by Hinderks et al. (2020), who propose a structural HJM-framework that is consistent with the initial forward price curve, and in which options on futures can be efficiently priced in the various model specifications.

Market coupling and the role played by interconnectors have also been the subject of several studies in recent years. Parisio and Bosco (2008) introduce a setup with equilibrium bid functions in individual domestic markets. They study the way these functions are affected when cross-border trading is managed using the implicit auction method, and analyse the effect of this mechanism on price convergence. With a particular focus on Italy, Pellini (2012) evaluates the impact on the Italian electricity market of replacing an explicit auction mechanism with an implicit one, i.e., with market coupling, and shows that the effects on welfare and social surplus are likely to be positive. Cartea and González-Pedraz (2012) take a real options approach to determine the value of an interconnector. They study five pairs of neighbouring European markets, determine the values of the interconnectors for each pair over a one-year period in their setup, and find that jumps in price spreads can have a significant impact on these values. Füss et al. (2017) employ a fundamental multi-market model to study electricity spot and derivatives pricing under market coupling, and analyse how the behaviour of these prices depends on different cross-border allocation schemes. Kiesel and Kustermann (2016) calibrate their structural model to the French-German market area and study the effect of market coupling on electricity prices and the value of power plants. They find that market coupling can lead to lower futures prices in all affected markets, even the cheapest one, and can also result in volatility spillover effects. Pircalabu and Benth (2017) combine regime-switching with a copula model for a pair of electricity prices. Each hour is considered independently of the others, and pricing is performed using a Monte Carlo simulation. Their empirical study is based on four pairs of market areas, for which they find significant evidence of tail dependence in the interconnected areas considered. Parisio and Pelagatti (2019) focus on the market coupling between Italy and Slovenia, and assess the degree of integration between these markets arising because of this policy. They find that despite this existing link, the two markets are still far from being strongly integrated. Cartea et al. (2019) analyse an investor's optimal strategy when trading electricity contracts in two interconnected locations. They show that as his aversion to ambiguity increases, his trading activity, and consequently his inventory exposure, decreases in both locations. Christensen and Benth (2020) introduce regime-switching in their model for potentially coupled electricity prices using a latent uni-variate process that allows for seasonal behaviour. The parameters of this process are estimated from given market data via particle filtering. They show that their model can be used for the analytical pricing of forwards and spread options, and illustrate its performance in a case study of the French and German markets. Schrader and Benth (2022) consider the new NordLink cable between Germany and Norway, and analyse the effect that the exchange of power production between two countries can have on carbon emissions. They conclude that the cable can be used as an effective way to reduce carbon emissions by exporting surplus German renewable production to Norway on windy days, and importing surplus Norwegian energy production to Germany on non-windy days.

In this article, we take the Cartea and González-Pedraz (2012) modelling framework as our point of departure, and set out from there to take the aforementioned developments in market coupling and interconnectors into account. One such development is the finer granularity in electricity markets. Cartea and González-Pedraz (2012) consider the means of day-ahead prices (also called spot prices) over peak and off-peak hours when pricing interconnector options. In practice, however, these options are strips of individual options for each hour of the day. This distinction is important, because the dynamics of the hourly spreads are quite different from the dynamics of the spreads of mean spot prices. In fact, due to the physical constraints of the connection, the hourly spread is either equal to zero if there is enough capacity to allow the same price in the two locations, or different from zero if the lines are overloaded. To account for these network constraints, we propose a formulation of the problem with regime-switching for the underlying hourly spreads. We note that our reduced-form model is highly tractable and allows for robust parameter estimation. As we will show, prices of interconnector options can be computed in closed-form. Another even more recent development is the dramatic paradigm shift in European electricity markets that began in the summer of 2021. Drawing on our data set, which starts in 2017, we illustrate the strong effect of this shift on the model parameters. Finally, we consider the issues of

reliably pricing and trading spread options in such a volatile and uncertain market environment.

Main contributions

Our main contributions are:

- We increase the resolution from daily (peak, off-peak) electricity prices to hourly prices, and add regime-switching to reflect coupled and decoupled hours.
- We perform a simulation exercise to demonstrate that our regime-switching model successfully captures the important stylised features of intermittently connected markets.
- We show that our model can adapt to the new market paradigm of high prices, uncertainty and volatility.
- We find that the pricing of spread options works well in a "normal" market environment. However, in a highly volatile environment, both auction and model *ex ante* spread option prices may turn out to lie far from *ex post* realised payoffs.

Structure of the article

The remainder of the article is organised as follows. In Section 2, we describe the current European interconnector market. In Section 3, we present our model, which is based on the Cartea and González-Pedraz (2012) model and a 2-state Markov process that describes regime-switching between coupled and decoupled periods in the market. Section 4 explains how to estimate the model parameters for given hourly power prices from various European electricity markets. In Section 5, we show that our model can adapt to the new market paradigm that began in early autumn, 2021. Section 6 concludes the article. In Appendix A, we review Fourier transform methods for the pricing of European spread options.

2 The European Interconnector Market

2.1 An Interconnected European Electricity Market

The interconnection market in Europe allows market participants to buy or sell flows of energy between two locations in order to exploit price differentials between locations. These locations are delimited in Europe by the different Transmission System Operators (TSOs) and can be a country or a larger bidding area. For example, France (FR) has interconnections with Belgium (BE), Switzerland (CH), Germany (DE), Spain (ES) and Italy (IT).

Before the introduction of this market, a trading member had to first reserve cross-border capacity, before transporting the purchased electricity in a second step. The interconnection market simplifies the process via implicit auctions in which market participants simply bid for electricity on the exchange.

This auction market comprises both intra-day products and long-term options. When a participant buys an option in the DE→FR interconnection, for example, he buys the right to transit energy for each hour of the period considered from Germany to France. When the flux is financial, the payoff of such an option is:

$$\text{Payoff} = \sum_{h \in \mathcal{H}} \max\Big(S^A(h) - S^B(h) - K, 0\Big), \tag{1}$$

where K is the strike price, $S^c(h)$ is the spot price for each country $c = A, B$ at a given hour h, and $\mathcal{H}$ is the set of all hours in the period. The price of such an option is a function of the dynamics of

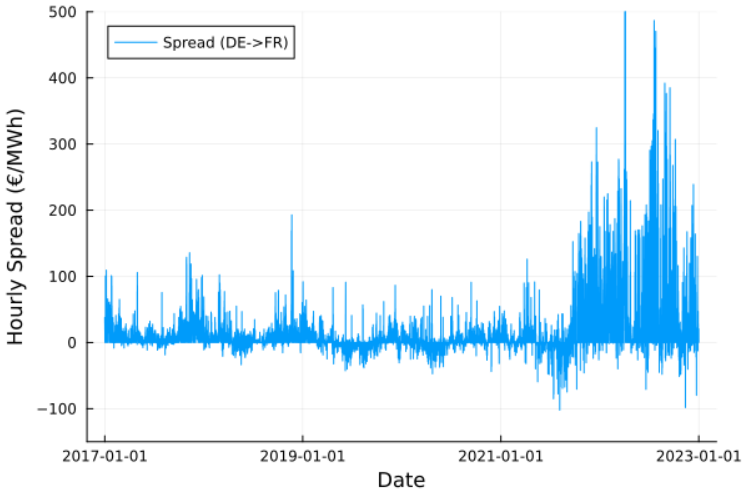

Figure 1: Price differences between France and Germany since 1 January 2017.

the underlying spread. Figure 1 displays the hourly spread $S^{FR,DE} = S^{FR} - S^{DE}$ used to value the DE→FR interconnection. We observe that during many hours in this period, electricity prices were higher in France than in Germany, leading to positive price spreads.

When electricity is sent from one country to another, the ensuing spread can be denoted in two ways that must not be confused: DE → FR means that electricity is sent from Germany (DE) to France (FR), which means that electricity is bought in DE and sold in FR, which leads to a spread of $S^{FR,DE} = S^{FR} - S^{DE}$. In the other direction, FR → DE means that electricity is sent from France to Germany, which means that electricity is bought in FR and sold in DE, leading to the opposite spread of $S^{DE,FR} = S^{DE} - S^{FR}$.

2.2 Market Coupling and Decoupling

In Europe, the day-ahead price is fixed by an algorithm called Euphemia and powered by European electric power exchange EPEX Spot. The algorithm allows us to take into account the Price Coupling Regions (PCR) by optimising the maximal welfare with the interconnection constraints. The efficiency of market coupling is proven by an increasing price convergence between market areas. As a consequence, when the interconnection lines between two countries for a given hour are not saturated, the price is the same for both, which means that the spread is zero. In this case we say that the market is *coupled*. In contrast, when there is insufficient capacity and prices differ, we say that the market is *decoupled*.

If we take Figure 1 and zoom in over a shorter period, for example May 2018, as shown in Figure 2, we observe that there are many occasions when the hourly spread is zero. In this example, 20% of the DE and FR hours are coupled, with an ensuing price spread of zero.

This situation is similar for other European interconnections. Table 1 shows German (DE) hourly

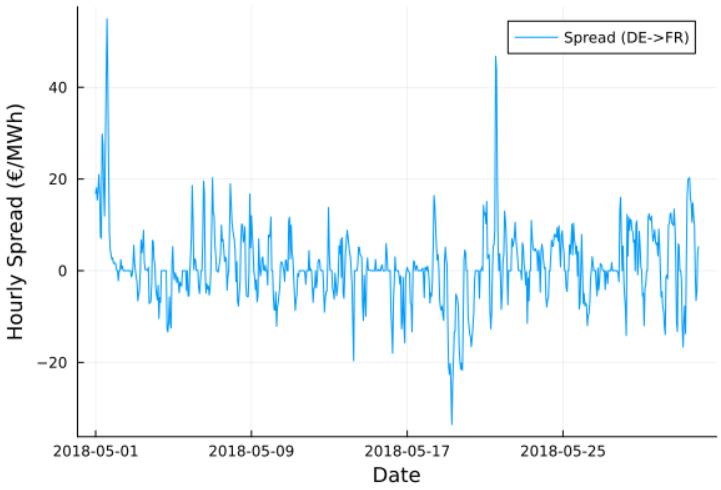

Figure 2: Hourly price differences between France and Germany in May 2018.

market price spreads with neighbouring countries for 24 May 2022 from EPEX Spot. We can see that at the beginning of the day, in hours 1 to 3, all German spreads are different from zero, meaning that Germany is completely decoupled from its neighbours. Then, for most of the day, some countries are coupled with Germany, while others are not. Finally, in hours 21 to 23, all German spreads are equal to zero, meaning that Germany is completely coupled with its neighbours.

The situation can change if we consider daily rather than hourly price spreads. To illustrate the different behaviour of hourly and daily spreads in the market, Figure 3 shows the daily spread in the first half of 2018. Due to the averaging of the hourly prices over the day, and since there are virtually no days on which all 24 hours are coupled, the coupled regime disappears, and only the decoupled regime is observed. The periods over which price spreads are calculated when determining the payoff of an interconnection option are therefore an important contractual specification.

To understand the importance of these periods, let us take a closer look at the price spreads observed in the market between Germany and Poland shown in Table 1. The sum of the spreads over the eight peak hours from 9 to 20 in column DE→PL is −121.56 (in EUR/MWh), or −10.13 per hour, on average. For the remaining off-peak hours from 1 to 8 and 21 to 24, the sum of the spreads is −155.74, or −12.98 per hour. Finally, over the whole day, the total base spread is −277.30, or −11.55 per hour. In all three cases, i.e., peak, off-peak and base load, the payoff of an interconnection option with strike $K = 0$ is equal to zero, since the three spreads are negative. This changes, however, if we look at an interconnection option whose payoff is based on each hour individually. The spreads for the hours 1 to 3 and then again 14 to 20 are positive, and when we calculate the payoff of this hourly option using equation (1), we obtain a positive payoff of EUR 186.02. Table 2 compares these different option payoffs for the couple DE→PL just discussed, as well as the other country couples of Table 1. The couple DE→PL stands out, of course, because of its pronounced alternation between positive and negative price spreads.

Table 1: German (DE) price spreads with neighbouring countries for 24 May 2022

HOUR	DE → AT	DE → BE	DE → FR	DE → NL	DE → PL	DE → CZ
1	20.97	69.21	80.93	137.93	16.34	16.34
2	21.25	48.02	82.91	93.75	21.25	21.25
3	23.61	42.88	72.68	75.93	15.55	15.55
4	17.46	33.28	48.64	41.76	0	0
5	8.35	20.2	29.64	25.43	0	0
6	0	0	0	0	-37.58	0
7	0	0	0	0	-60.36	0
8	0	0	0	0	-95.82	0
9	0.66	-2.04	2.86	-1.88	-89.47	0.66
10	0	0	0	0	-70.51	0
11	4.6	-3.11	0.13	-3.7	-60.27	4.6
12	16.64	0	6.11	0	-32.75	16.64
13	19.54	0	50.83	0	-1.44	19.54
14	32.45	0	50.69	0	11.92	32.45
15	35.5	0	50.9	0	32.7	35.5
16	15.86	0	10.95	0	15.86	15.86
17	7.6	-4.28	0	-4.28	7.6	7.6
18	13.57	-7.65	-1.71	-6.19	23.52	23.52
19	0	0	0	0	10.83	0
20	0	0	0	0	30.45	0
21	0	0	0	0	0	0
22	0	0	0	0	0	0
23	0	0	0	0	0	0
24	0	0	0	0	-15.12	0

Table 2: Interconnection option payoffs for 24 May 2022

Method	DE → AT	DE → BE	DE → FR	DE → NL	DE → PL	DE → CZ
Peak	146.42	0	82.91	0	0	156.37
Off-Peak	91.64	213.41	314.80	374.80	0	53.14
Base	238.06	196.33	485.56	358.75	0	209.51
Hourly	**238.06**	**213.41**	**487.27**	**374.80**	**186.02**	**209.51**

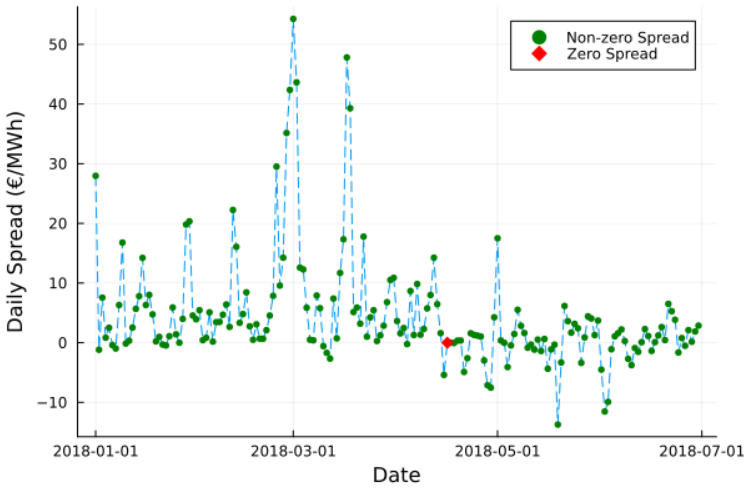

Figure 3: Daily price differences between France and Germany in the first half of 2018. The daily spread was only equal to zero on 16 April 2018.

2.3 Electricity Spreads and Spread Options

Let $S^A(t)$ and $S^B(t)$ at time t be electricity spot prices in locations A and B, respectively, and define their spread as:

$$S^{A,B}(t) = S^A(t) - S^B(t)$$

namely, the difference between these two prices. Let r be the continuously-compounded risk-free interest rate. The model price of a single call option with strike $K^{A,B}$ at an hour T is given by the discounted expected payoff:

$$C^{A,B}(t, T, K^{A,B}) = e^{-r(T-t)}\mathbb{E}_t\left[\max(S^{A,B}(T) - K^{A,B}, 0)\right],$$

and the value of the monthly option is then given by:

$$C_M^{A,B}(t, K^{A,B}) = \sum_{T=T_1}^{T_N} C^{A,B}(t, T, K^{A,B}),$$

where T_1,..., T_N are the hours of delivery in month M. In practice, the strike $K^{A,B}$ is usually set to zero. However, we consider the more general case of any strike value here. Non-zero values of the strike could be taken to account for possible interconnection costs, for example.

As usual in electricity markets, option prices are quoted per MWh. To obtain the actual price of the option, this price needs to be multiplied by the number of hours in the month.

If the characteristic function of the spread $S^{A,B}(T)$ is available, but the probability density is not, option valuation theory allows us to use the Fourier-transform (see Carr and Madan (1999)) to numerically compute the price of such a spread option.

3 An Interconnector Model with Regime Switching

3.1 The Cartea-González-Pedraz Model

We begin the description of the interconnector model by recalling the main features of the Cartea and González-Pedraz (2012) model. They propose the following model for electricity spreads under the physical probability measure $\mathbb{P}$. Let $(\Omega, \mathcal{A}, \mathbb{P}, \mathcal{F})$ be a filtered probability space. Let $S^A(t)$ and $S^B(t)$ be electricity spot prices at time t in locations A and B, respectively, and define their spread as:

$$S^{A,B}(t) = S^A(t) - S^B(t), \tag{2}$$

i.e., the difference between these two prices. Cartea and González-Pedraz (2012) assume that this spread follows an arithmetic model given by:

$$S^{A,B}(T) = f(T) + X(T) + Y(T). \tag{3}$$

The seasonality function f describes a deterministic seasonal pattern. The process X is an Ornstein-Uhlenbeck process given by:

$$X(T) = X(t)e^{-\alpha(T-t)} + \int_t^T e^{-\alpha(T-s)}\sigma(s)dB(s) \tag{4}$$

with mean-reversion speed $\alpha > 0$ and volatility $\sigma > 0$, and where $B = (B_t)_{t\geq 0}$ is a standard $\mathcal{F}$-adapted Brownian motion under $\mathbb{P}$. The process Y is a zero-mean-reverting pure jump process given by:

$$Y(T) = Y(t)e^{-\beta(T-t)} + \int_t^T e^{-\beta(T-s)}dJ^+(s) + \int_t^T e^{-\beta(T-s)}dJ^-(s). \tag{5}$$

with mean-reversion speed $\beta > 0$ and jump-intensities $\lambda^+, \lambda^- \geq 0$. In the general formulation of the model, these jump-intensities can be time-dependent. Here, for simplicity and better tractability, we assume that these parameters are constant.

The compound Poisson processes J^+, J^- are given by:

$$J^+(t) = \sum_{n=1}^{N^+(t)} j_n^+, \tag{6}$$

$$J^-(t) = \sum_{n=1}^{N^-(t)} j_n^-, \tag{7}$$

where $N^+(t), N^-(t)$ are Poisson processes with intensities $\lambda^+ and \lambda^-$, respectively. The variables j^+ and j^- denote positive and negative jumps, which are exponentially i.i.d. with parameters $\eta^+, \eta^- > 0$. The expected jump sizes are therefore $1/\eta^+$ and $1/\eta^-$.

As is shown in Cartea and González-Pedraz (2012), the characteristic function $\phi_T = \phi_{S^{A,B}(T)}$ of $S^{A,B}(T)$ is given for $u \in \mathbb{R}$ by:

$$\phi_T(u) = \exp\left(iuh(T) - \frac{1}{4\alpha}u^2\sigma^2(1-e^{-2\alpha T})\right) \cdot \left(\frac{\eta^+ - iue^{-\beta T}}{\eta^+ - iu}\right)^{\lambda^+/\beta} \cdot \left(\frac{\eta^- + iue^{-\beta T}}{\eta^- + iu}\right)^{\lambda^-/\beta}, \tag{8}$$

with

$$h(T) = f(T) + e^{-\alpha(T-t)}X(t) + e^{-\beta(T-t)}Y(t).$$

Note that ϕ_T has singularities at $u = -i\eta^+$ and $u = i\eta^-$.

3.2 Regime Switching via a Two-State Markov Process

Let $\mathcal{S} = \{0, ..., m-1\}$ be a finite state space for a Markov process $M = (M_t)_{t\geq 0}$ in continuous time on a probability space $(\Omega, \mathcal{A}, \mathbb{P})$. Let the $m \times m$-matrix $Q = (q_{ij}), q_{ij} \in \mathbb{R}\ \forall i, j \in \mathcal{S}$, satisfy the following conditions:

1) $q_{ij} \geq 0\ \forall i, j \in \mathcal{S}$ with $i \neq j$; $\quad q_{ii} \leq 0\ \forall i \in \mathcal{S}$,

2) $\sum_{j\in S} q_{ij} = 0\ \forall i \in \mathcal{S}$, (rows sum to zero)

3) $0 < \max_{i\in S} |q_{ii}| < \infty$.

The matrix Q is called the *infinitesimal generator* of the process M.

The transition probability matrices $P(t)$ are given for $t \geq 0$ by the matrix exponential:

$$P(t) = e^{tQ} = \sum_{n=0}^{\infty} \frac{(tQ)^n}{n!}. \tag{9}$$

The *stationary distribution* is defined by $\pi Q = 0$. It also satisfies $\pi P(t) = \pi$ for all $t > 0$.

Assume that $m = 2, \mathcal{S} = \{0, 1\}$, i.e., that the Markov process M has the two states 0 and 1. In this case, we simplify the notation and refer to the off-diagonal elements of Q as q_0 and q_1, so that $q_{00} = -q_0, q_{01} = q_0, q_{10} = q_1, q_{11} = -q_1$. We assume that $0 < q_0, q_1 < \infty$. The generator Q is given by:

$$Q = \begin{pmatrix} q_{00} & q_{01} \\ q_{10} & q_{11} \end{pmatrix} = \begin{pmatrix} -q_0 & q_0 \\ q_1 & -q_1 \end{pmatrix}.$$

Using Kolmogorov's backward equation (Stroock, 2005):

$$P'(t) = QP(t),$$

with:

$$P(t) = \begin{pmatrix} p_{00}(t) & p_{01}(t) \\ p_{10}(t) & p_{11}(t) \end{pmatrix}$$

it can be shown that:

$$p_{00}(t) = \frac{q_1}{q_0 + q_1} + \frac{q_0}{q_0 + q_1} e^{-(q_0+q_1)t}, \tag{10}$$

$$p_{01}(t) = \frac{q_0}{q_0 + q_1} - \frac{q_0}{q_0 + q_1} e^{-(q_0+q_1)t}, \tag{11}$$

$$p_{10}(t) = \frac{q_1}{q_0 + q_1} - \frac{q_1}{q_0 + q_1} e^{-(q_0+q_1)t}, \tag{12}$$

$$p_{11}(t) = \frac{q_0}{q_0 + q_1} + \frac{q_1}{q_0 + q_1} e^{-(q_0+q_1)t}. \tag{13}$$

Note that we have $p_{00}(t) + p_{01}(t) = 1$ and $p_{10}(t) + p_{11}(t) = 1$, which is natural from a Markov chain point of view. Note also that for the sum of the *diagonal probabilities* we have the condition:

$$p_{00}(t) + p_{11}(t) > 1, \tag{14}$$

and for the sum of the *off-diagonal probabilities* we have the condition:

$$p_{01}(t) + p_{10}(t) < 1. \tag{15}$$

Conversely, if the transition matrix $P(t)$ is given for some $t > 0$ and satisfies the restrictions (14) and (15), then the generator Q can be calculated from it as follows. This will be useful for estimating the parameters of the Markov process M.

Adding equations (11) and (12) gives:

$$p_{01}(t) + p_{10}(t) = 1 - e^{-(q_0+q_1)t},$$

and therefore:

$$q_0 + q_1 = -\frac{1}{t}\ln(1 - p_{01}(t) - p_{10}(t)). \tag{16}$$

Now, substituting (16) in (11) and (12), respectively, gives:

$$q_0 = -\frac{1}{t}\ln(1 - p_{01}(t) - p_{10}(t)) \cdot \frac{p_{01}(t)}{p_{01}(t) + p_{10}(t)} \tag{17}$$

$$q_1 = -\frac{1}{t}\ln(1 - p_{01}(t) - p_{10}(t)) \cdot \frac{p_{10}(t)}{p_{01}(t) + p_{10}(t)} \tag{18}$$

The stationary distribution, satisfying $\pi Q = 0$, is given by $\pi = (\frac{q_1}{q_0+q_1}, \frac{q_0}{q_0+q_1})$.

3.3 An Interconnector Model with Regime Switching

We now combine the Cartea and González-Pedraz (2012) model of Section 3.1 with the Markov regime-switching process of Section 3.2.

Let $S_0 = (S_{0,t})_{t\geq 0}$ and $S_1 = (S_{1,t})_{t\geq 0}$ be two stochastic processes defined over the same probability space as the Markov process M. Further, we assume that S_0 and S_1 are both independent of the process M. We define the regime-switching process S as:

$$S(t) = S_0(t)\mathbb{I}_{\{M_t=0\}} + S_1(t)\mathbb{I}_{\{M_t=1\}}. \tag{19}$$

The characteristic function $\phi_{S_T} = \phi_T$ of $S(T)$ is then given for $u \in \mathbb{R}$ by:

$$\begin{aligned}
\phi_T(u) &= E[e^{iuS(T)}] \\
&= \mathbb{P}(M_T = 0)E[e^{iuS(T)}|M_T = 0] + \mathbb{P}(M_T = 1)E[e^{iuS(T)}|M_T = 1] \\
&= \mathbb{P}(M_T = 0)E[e^{iuS_0(T)}] + \mathbb{P}(M_T = 1)E[e^{iuS_1(T)}] \\
&= \mathbb{P}(M_T = 0)\phi_{0,T}(u) + \mathbb{P}(M_T = 1)\phi_{1,T}(u),
\end{aligned}$$

where $\phi_{0,T}$ and $\phi_{1,T}$ are the characteristic functions of $S_0(T)$ and $S_1(T)$, respectively.

The probability vector $\pi = (\pi_0, \pi_1)$, with $0 < \pi_0, \pi_1 < 1$ and $\pi_0 + \pi_1 = 1$, of the stationary distribution of the Markov chain satisfies the relationship:

$$\pi P(t) = \pi,$$

or, equivalently,

$$\pi Q = 0.$$

For the generator Q as given above, we obtain:

$$\pi = \left(\frac{q_1}{q_0 + q_1}, \quad \frac{q_0}{q_0 + q_1}\right).$$

In particular, note that π does not depend on time t.

We now come to the specification of the two regimes in our model. As we described in Section 2, the market switches between two regimes in which the spread $S^{A,B}(t) = S^A(t) - S^B(t)$ between electricity prices in two locations A and B at time t, as defined in equation (2), is either equal to 0 or different from 0. These are our regimes 0 and 1. We therefore specify that the process S_0 is constant and equal to 0, and that the process S_1 is the one proposed by Cartea and González-Pedraz (2012), i.e.:

$$S_0(t) \equiv 0, \tag{20}$$
$$S_1(t) = f(T) + X(T) + Y(T), \tag{21}$$

where $S_1(t) = S^{A,B}(t)$ is the process given in equation (3).

3.4 Spread Option Pricing

In the case of a monthly interconnection product, the option gives the right to dispatch electricity from location A to location B at each hour of the considered month. Thus the valuation of interconnection capacity between two locations is equivalent to evaluating a strip of European-style options, where the underlying is the spread price between the two countries. Let r be the continuously-compounded risk-free interest rate. The price at time t of a call option on the spread $S^{A,B}$ at a single hour T is given by:

$$C^{A,B}(t, T, K^{A,B}) = e^{-r(T-t)}\mathbb{E}_t\left[\max(S^{A,B}(T) - K^{A,B}, 0)\right].$$

It follows that the value of a monthly call option on the spread $S^{A,B}$ during the month M is then given by:

$$C_M^{A,B}(t, K^{A,B}) = \sum_{T=T_1}^{T_N} C^{A,B}(t, T, K^{A,B}),$$

where T_1,..., T_N are the hours of delivery in this month.

Using the model's characteristic function ϕ, the price of the call option can be evaluated as:

$$C^{A,B}(t, T, K^{A,B}) = -\frac{1}{2\pi}\int_{-\infty-i\alpha}^{\infty-i\alpha} e^{-izK}\frac{1}{z^2}\phi(z)dz.$$

These results are well-known and stated for completeness in Appendix A.

We also have a parity between call options on spreads in opposite directions with opposite strikes. Let $C^{A,B}(t, T, K)$ and $C^{B,A}(t, T, -K)$ be two call options with the same maturity T on the opposite spreads $S^{A,B}(T)$ and $S^{B,A}(T)$ with opposite strikes K and $-K$. Their present values are then given by the expressions:

$$C^{A,B}(t, T, K) = e^{-r(T-t)}\mathbb{E}_t\left[\max(S^{A,B}(T) - K, 0)\right],$$
$$C^{B,A}(t, T, -K) = e^{-r(T-t)}\mathbb{E}_t\left[\max(S^{B,A}(T) + K, 0)\right].$$

Observe that the call option $C^{B,A}(t, T, -K)$ with strike $-K$ can also be seen as a put option $P^{A,B}(t, T, K)$ with strike K, since:

$$\mathbb{E}_t\left[\max(S^{B,A}(t) + K, 0)\right] = \mathbb{E}_t\left[\max(K - S^{A,B}(t), 0)\right].$$

We therefore have, from standard call-put parity:

$$C^{A,B}(t, T, K) - C^{B,A}(t, T, -K) = e^{-r(T-t)} \cdot (\mathbb{E}_t\left[S^{A,B}(T)\right] - K).$$

4 Model Calibration and Estimation

4.1 Our Data Set

Our data set covers the period from 1 January 2017 to 31 August 2022 and comprises three types of data:

1) European hourly electricity prices from the European Power Exchange (EPEX-SPOT): `https://www.epexspot.com/en/market-data`

2) European monthly futures prices from the European Energy Exchange (EEX): `https://www.eex.com/en/market-data/power/futures`

3) European monthly auction prices from the Joint Allocation Office (JAO): `https://www.jao.eu/auctions/`

Note that while the historical data from the EPEX-SPOT are only provided on a subscription basis, data from the EEX and JAO are public and freely available on the internet websites given above.

The behaviour of electricity prices in European wholesale markets has changed significantly in recent years. Figure 4 illustrates this change, beginning around September 2021, with the example of the DE→FR spread between France and Germany. Post-covid Chinese economic revival, the European gas crisis caused by the war in Ukraine, low electricity production in France due to maintenance issues with nuclear power plants, an especially hot summer in 2021 - all of these factors have wrought profound changes in the equilibrium of commodity markets and have led to large increases in price levels and market volatility.

Our article does not attempt to provide a detailed explanation of the new fundamentals underlying this paradigm change. However, in order to estimate our model, we need to take these changes into account. We therefore split our data set into two parts:

1) from 1 January 2017 to 31 August 2021;

2) from 1 September 2021 to 31 August 2022.

From now on, we also refer to these two parts of our original data set as *data set 1* and *data set 2*, respectively, in order to simplify our terminology.

Table 3 summarises the model parameters to be estimated. Note that we estimate them in the order given in the table, from top to bottom.

Parameter	Role
q_0, q_1	infinitesimal generator Q of Markov regime-switching process M
λ^+, η^+	intensity and inverse mean of upward jumps J^+
λ^-, η^-	intensity and inverse mean of downward jumps J^-
α, σ	mean-reversion and volatility of Ornstein-Uhlenbeck process X
β	mean-reversion of pure jump process Y

Table 3: Model Parameters.

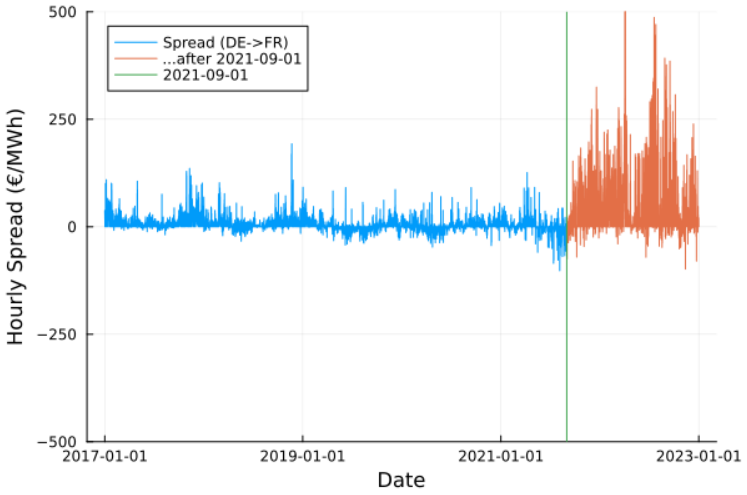

Figure 4: Spread DE→FR before and after September 2021.

4.2 Specifying and Estimating the Seasonality Function

It is well known that electricity prices are seasonal at several frequencies, such as daily, weekly, monthly, and yearly. Accordingly, seasonality functions are an important topic in the literature; see, for example, Lucia and Schwartz (2002) and Cartea and Villaplana (2008) for discussions and various specifications.

Seasonality is less of an issue for electricity price spreads between neighbouring countries, the case considered in this article. Most of the European countries studied here are in the same time-zone and share many consumption patterns. Seasonal fluctuations therefore tend to cancel out to a large degree. And of course, as periods of market coupling increase between countries, the importance of seasonality diminishes even further, since it plays no role during coupled periods.

Moreover, the market only provides information on forward prices, which are given at a monthly granularity at the moment of the auctions. Therefore, when pricing monthly spread options, we only have a constant view of the spread for the given period. To be consistent with the pricing in the calibration procedure, we therefore shift the process by a constant whose value is simply given by the mean of the historical spread process in the data set. Since we account for regime switching of market coupling, we only consider this component during decoupled periods.

As described above, when we price spread options, we will use the market forward price that is appropriate for the option period. For example, when pricing monthly spread options, we will take the difference of the two monthly forward prices of the countries in question as input. In our model, we have:

$$f(T) = \pi_0 f_0(T) + \pi_1 f_1(T).$$

We assume $f_0(T) = 0$ for all T. Therefore, in order for the model to reproduce the market forward $f(T)$ for time T, we set:

$$f_1(T) = \frac{1}{\pi_1} f(T).$$

4.3 Estimating the Transition Probabilities of the Markov Process

We continue the description of our multi-step estimation procedure by estimating the transition probabilities of the Markov process M introduced in Section 3.2.

First we need to identify the switches between the two regimes represented by $M(t) = 0$ and $M(t) = 1$. This step allows us to estimate the infinitesimal generator Q of the Markov process M. Note that this first step is directly based on the spread data and is therefore simple and stable.

Let $N_{i\to j}$ denote the number of times the process switches from state i to state $j \neq i$, and let N_i denote the number of steps spent in state i. We can then estimate the 1-hour transition probabilities as:

$$p_{01} = p_{01}(1 \text{ hour}) = \frac{N_{0\to 1}}{N_0}, \tag{22}$$

$$p_{10} = p_{10}(1 \text{ hour}) = \frac{N_{1\to 0}}{N_1}, \tag{23}$$

which, using equations (17) and (18), gives us the estimates:

$$q_0 = -\ln(1 - p_{01} - p_{10})\frac{p_{01}}{p_{01} + p_{10}}, \tag{24}$$

$$q_1 = -\ln(1 - p_{01} - p_{10})\frac{p_{10}}{p_{01} + p_{10}}, \tag{25}$$

for the entries $q_0 = q_{01} = -q_{00}$ and $q_1 = q_{10} = -q_{11}$ of the matrix Q. Note that the coefficient $\frac{1}{t} = 1$ in this case, since our unit of time is one hour. This estimation of the parameters of the infinitesimal generator Q completely describes the behaviour of the Markov process M over time.

Interconnection	**DE→FR**	
Start Date	01/01/2017	01/09/2021
End Date	31/08/2021	31/08/2022
p_{01}(1 hour)	0.1760	0.1817
p_{10}(1 hour)	0.1278	0.1109
q_0	0.2098	0.2150
q_1	0.1523	0.1312

Table 4: Transition probabilities of the Markov process M.

Table 4 shows the parameters describing the Markov process M. In the first data set, the probability of switching from the coupled regime 0 to the uncoupled regime 1 is estimated to be $p_{01} = 17.60\%$ per hour. This means that the expected length of staying in the coupled regime is $p_{01}^{-1} = 5.68$ hours. For the second data set, this length decreases slightly to $0.1817^{-1} = 5.50$ hours. In the other direction, in the first data set, the probability of switching from the uncoupled regime 1 to the coupled regime 0 is 12.78% per hour, which translates into an expected length of staying in the uncoupled regime of $0.1278^{-1} = 7.82$ hours. For the second data set, this length increases slightly to $0.1109^{-1} = 9.02$ hours. Note that the transition probabilities remain relatively stable over the two data sets. We will see shortly that this is not at all the case for most of the other model parameters.

Figure 5 highlights the times at which regime switching occurs for the price spread between France and Germany in the first days of January 2020. The plotted spreads are in line with the random behaviour of the regime switching described in Table 4. In the first week, four longer periods of coupled markets can be observed, as well as one long period of decoupled markets. However, towards the end of the period shown, there is more frequent regime-switching, and only one slightly longer period of uncoupled markets can be seen.

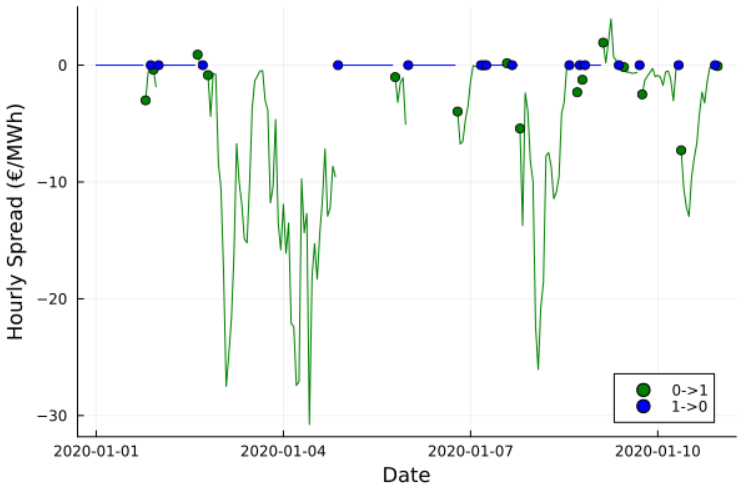

Figure 5: Identification of regime switching moments (spread DE→FR).

4.4 Detecting Jumps and Estimating their Intensity and Distribution

The goal of this section is to estimate the parameters λ^+, η^+ and λ^-, η^-, which describe the intensity and inverse mean of the upward and downward jumps J^+ and J^- given in equations (6) and (7), respectively. The remaining mean-reversion parameter β, needed to completely describe the pure jump process Y given in equation (5), will be estimated in the following Section 4.5.

In the previous Section 4.3, we identified the state of the Markov process M at all times (hours) t in our sample. We remove all t for which $M(t) = 0$, i.e., $S(t) = S_0(t) = 0$, from our spread series $S(t)$ in order to focus on the estimation of the parameters of the process S_1 from now on.

In this new, reduced series, however, we want to avoid counting spurious jumps that result from gluing the series together after having taken out an interval during which $S(t) = 0$. For example, let us assume that the last time the series is in state 1 before a regime switch $1 \to 0$ is t_i, and then again the first time the series is in state 1 after a regime switch $0 \to 1$ is t_j; then, after removing the data points for times $t_{i+1}, ..., t_{j-1}$ from our series, we tag the price move from $S(t_i)$ to $S(t_j)$ as an invalid candidate for a jump.

Figure 6 illustrates the process with these points removed. In the upper graph, we have marked in red the "false" jumps, caused by regime-switching, that we wish to exclude from the estimation of the jump process Y. In the lower graph, we show the sequence of price spreads for which we are actually going to estimate the jump parameters λ^+, η^+ and λ^-, η^-.

Detecting potential jumps

To detect big price movements and potential jump-times, and then determine whether such a big movement is really due to a jump or whether it is only an effect of mean-reversion, we follow the methodology presented in Cartea and González-Pedraz (2012).

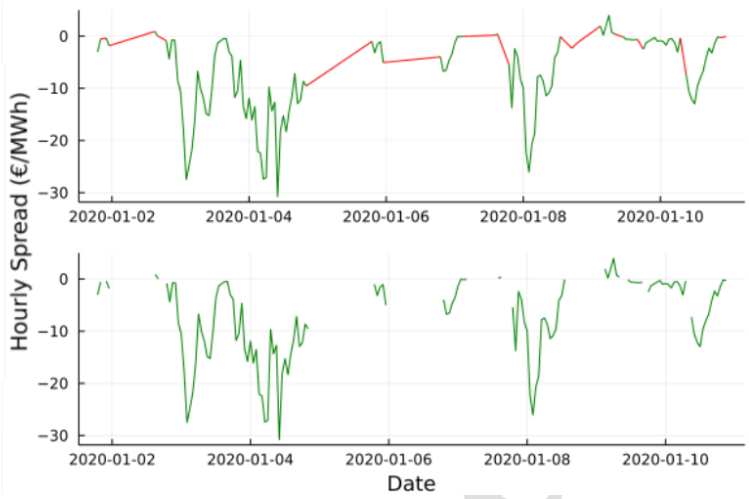

Figure 6: Process netted of points from regime switching.

We apply a recursive semi-parametric filter to identify the calendar position of the jumps in the price spread. The procedure identifies the hypothetical arrival of a jump when the spread difference deviates, in absolute value, by more than three standard deviations from its mean. It is therefore dependent on the length of the estimation time-windows.

Figure 7 highlights the jumps we identified for the DE→FR spread in the first half of 2020, during the estimation procedure for the first part of our data set (from 01/01/2017 to 31/08/2021).

Estimating jump intensities and jump size parameters

Once we have identified all up- and down-jumps in our time series, we need to identify the respective intensities λ^+ and λ^- of the Poisson processes N^+ and N^- appearing in the jump process Y. We do this by determining the frequency with which the jumps occur. We then fit two exponential distributions for the size of up- and down-jumps in the jump process Y.

The price spread is highly unbalanced in the second part of our data set, with French electricity prices almost always lying above German ones. Consequently, our estimation procedure does not detect any downward jumps; downward moves of the spread are entirely due to mean-reversion. We conclude that the jump process Y only allows for upward jumps.

Our results are shown in Table 5. Regarding the first part of our data set, we see that the frequency λ^+ of positive jumps is higher than the frequency λ^- of negative jumps. Also, the average size of positive jumps is $0.0433^{-1} = 23.09$ and slightly greater in magnitude than the average size of negative jumps, $0.0461^{-1} = 21.69$. This observation is exacerbated in the second part of our data set, where all jumps are positive, and their size is now $0.0030^{-1} = 333.3$ on average.

Figure 8 shows the probability density functions of the exponential distributions for the values of η^+ and η^- given in Table 5. It can be clearly seen that the density for the second data set has a much fatter tail to the right.

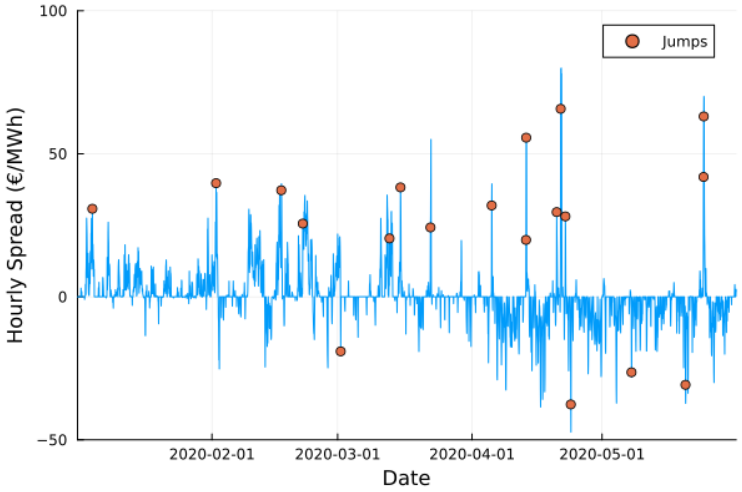

Figure 7: Jumps identified in the estimation procedure.

Interconnection	**DE→FR**	
Start Date	01/01/2017	01/09/2021
End Date	31/08/2021	31/08/2022
λ^+	0.0114	0.0031
λ^-	0.00252	0.0
η^+	0.0433	0.0030
η^-	0.0461	–

Table 5: Parameters of the compound Poisson processes J^+ and J^-.

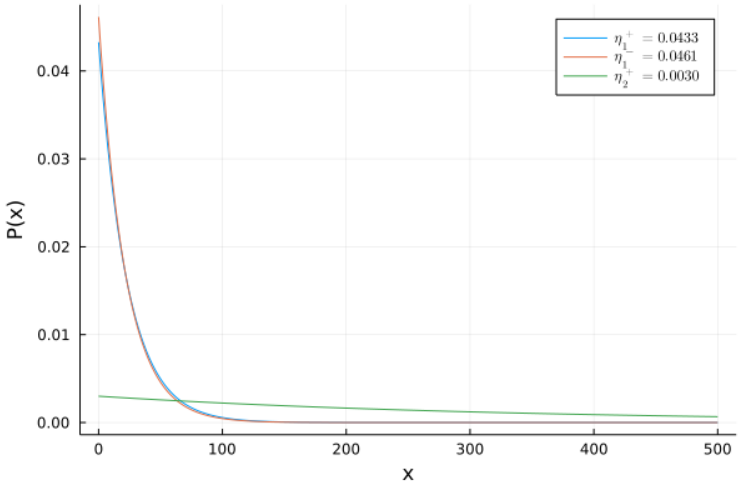

Figure 8: Exponential densities for both data sets.

4.5 Estimating the Mean-Reversion Speeds and Volatility

In order to conclude our estimation of the model parameters, we need to estimate the parameters α and σ, which describe the Ornstein-Uhlenbeck process X given by equation (4), as well as the parameter β, which describes the mean-reversion speed of the pure jump process Y given by equation (5).

We proceed by minimising the mean of the squared differences between observed and modelled spreads. There is, however, a difficulty, since it is not possible to observe the realised time series followed by X and Y individually, but only their sum $X+Y$. We therefore first fix the mean reversion parameter β of the process Y, and then apply the least-squares method to find the parameters α and σ of the process X implied for this value of β. We then repeat this step until we find the optimal value for the parameter β, and therefore the overall optimal triplet α, σ and β.

Table 6 shows the results for the spread DE→FR for both calibration windows. The mean reversion speeds α and β are relatively stable over the two data sets. However, the estimated volatility σ of the second time window is almost 10 times higher than that of the first one. We will see in Section 5.1 below that similar, if not quite so extreme, increases in volatility also hold for other pairs of neighbouring countries.

Interconnection	**DE→FR**	
Start Date	01/01/2017	01/09/2021
End Date	31/08/2021	31/08/2022
α	0.060	0.083
σ	4.506	43.632
β	0.100	0.100

Table 6: Mean reversion and volatility parameters of the processes X and Y.

5 Results

The first part of our results illustrates how dramatically electricity market conditions in Europe changed in 2021, and demonstrates that our model is capable of adapting to this new environment of high prices and volatility. The second part compares auction prices of monthly spread options from the past years to traded futures quotes and model prices for these options, and also to realised spreads during these periods.

5.1 A New European Paradigm

We begin with the regime-switching model estimated over data set 1, i.e., the period from 1 January 2017 to 31 August 2021. In Figure 9, we compare the realised price spread to a path that was simulated with the model. We see that our regime-switching model successfully captures the important stylised features of intermittently coupled markets:

1) two regime states, representing coupled and decoupled markets;

2) up- and downward jumps in the spread process;

3) a strong mean-reversion characteristic.

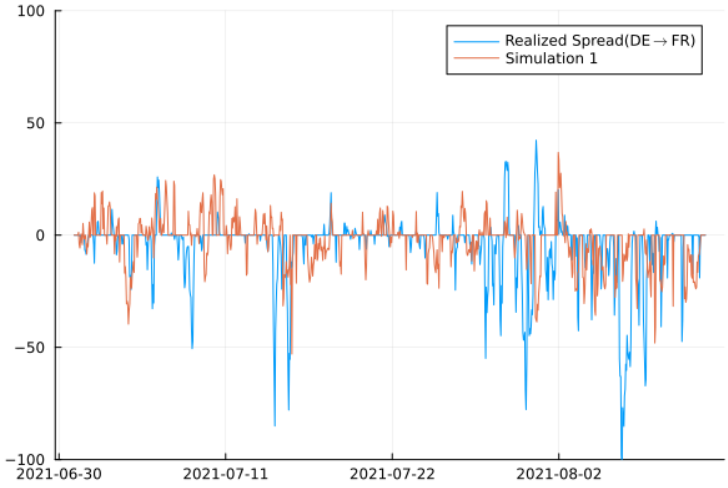

Figure 9: Comparison of realised and simulated price spreads for data set 1.

We also estimate the regime-switching model over data set 2, i.e., the period from 1 September 2021 to 31 August 2022. Our estimation procedure reveals a significant increase in the spread volatility σ. Table 7 presents estimated volatility parameters for all interconnections with Germany for both data sets. We see that the volatility of the spread has been multiplied by factors ranging from close to 3 (DE $\rightarrow$ BE, DE $\rightarrow$ NL, DE $\rightarrow$ PL) to almost 10 (DE $\rightarrow$ FR).

Table 7: German (DE) spread volatility σ with neighbouring countries for both data sets.

data set	DE → AT	DE → BE	DE → FR	DE → NL	DE → PL	DE → CZ
1	3.022	6.543	4.506	3.676	11.584	3.010
2	14.060	17.306	43.632	11.021	33.980	14.283

To graphically show this change in the market, Figure 10 presents three sample paths simulated for the first data set estimation on the left, and for the second data set on the right. We intentionally keep the same scale on both sides in order to highlight the radically different spread levels prevalent in the two data sets. The new paradigm in the electricity market can be clearly observed. Before the summer of 2021, as can be seen in the historical spreads on the top left, price spreads mostly stayed in the range of ± 50 EUR, with a few drops to around -100 EUR. After this time, as can be seen on the top right, price spreads frequently reach levels of 300 EUR, and the tenfold increase in volatility is easily visible.

Furthermore, the simulations show that our model is able to capture the unbalanced spread that we observe in the historical data. Note that although the estimated downward jump intensity λ^- is equal to zero for the second data set, we still observe negative spreads in the simulations on the right-hand side of Figure 10. This is because the continuous part of the spread process, X, is not defined individually for negative and positive spreads, and can therefore in itself lead to negative spreads.

5.2 A Comparison of Traded and Real Options

Table 8 compares market and model prices of monthly spread options for the country couple (DE, FR) in both directions. The market prices were obtained from the Joint Allocation Office (JAO) "Auctions" website. We also report monthly futures prices from the European Energy Exchange (EEX) for the closing date of the JAO auction for reference, together with their difference or spread. It is important to note that these spread option prices are auction prices, obtained from a 3-day bidding period and published on the closing date. The link between option prices and futures prices is therefore less direct here than in situations where option prices are real-time trading prices, and futures and options can be traded in synchrony.

Tables 9 and 10 show the profit-and-loss results of a trading strategy that simply makes bids for monthly spread options in the JAO auction at the model price. We assume here for simplicity that our bid does not alter the final auction price, which is reasonable if the volume is low compared to the total volume of interconnection exchange. Table 9 shows the results for the model estimated on the first data set, and Table 10 for the model estimated on the second data set. Naturally, in order to obtain proper out-of-sample results, we only use a model for bidding at auctions occurring after the end of the model's estimation period. If our bid succeeds in the auction, i.e., our model price is higher than the auction price, then we make a profit if the spread that is realised during the course of the calendar month is higher than the auction price at which we bought the option; otherwise, we make a loss. If our bid is too low and therefore not executed in the auction, we still compare the auction price to the realised spread and report whether our insufficient bid turned out to be right or wrong.

The analysis of our trading results is revealing and sheds further light on our findings about the "new European paradigm" in Section 5.1. Table 9 shows that the trading strategy executed with the model estimated for data set 1 is highly successful from September 2021 to August 2022: 20 out of 24 bids are made in the correct direction, and the overall profit is decidedly positive. However, with the market turmoil beginning in the summer of 2022, the situation reverses completely, and the trading strategy

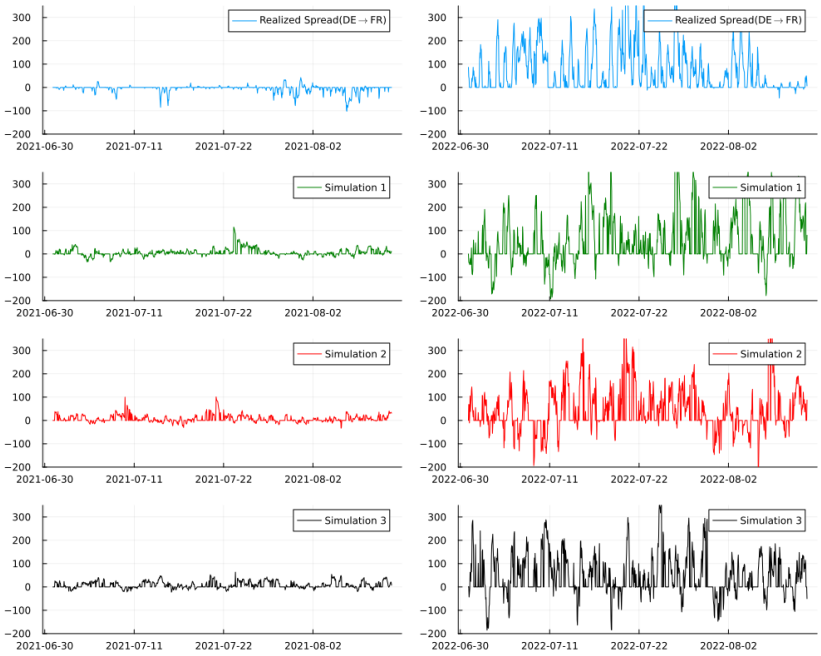

Figure 10: Comparison of realised and simulated price spreads for data set 1, on the left, and data set 2, on the right.

leads to injudicious bids and significant losses from September 2022 onwards. Interestingly, the trading outcome is essentially the same when we use prices from the model estimated on the more recent data set 2: bids are now also made for the direction FR → DE and lead to a slight loss; however, the bids in the more expensive direction DE → FR are unchanged and lead to the same losses as with the first model.

The finding that our model, used with two starkly differing sets of parameters, leads to essentially identical trading results is in part explained by the futures spreads of Table 8. These futures spreads turn out to be much higher than the realised spreads from September to December 2022. And since the futures spreads are a first-order input to the pricing model, it is a direct consequence that the model prices are also much higher than the realised spreads.

Finally, we can see from Tables 9 and 10 that from February 2023 onward, JAO auction prices have come down and realigned with the realised spreads. From February to August 2023, Model 1 performs marginally worse than Model 2 in the direction DE → FR (−6.95 vs −6.75 EUR), and slightly better (2.47 vs 1.98 EUR) in the direction FR → DE. Given that the realised spreads have decreased substantially in this period, we believe that it is necessary to regularly re-estimate model parameters on a rolling window basis. This allows us to work with a model that is a good fit with current market conditions and that can achieve positive trading results, as for example with Model 1 in the period before September 2022.

Table 8: Market and Regime-Switching Model Prices of Monthly DE-FR Spread Options in EUR/MWh

JAO Auction	Market Futures			JAO Options		Model 1	Model 2	Model 1	Model 2
Closing Date	DE	FR	Spread	DE→FR	FR→DE	DE→FR	DE→FR	FR→DE	FR→DE
22/09/21	135.07	154.26	19.19	18.27	1.08	20.44	-	0.21	-
25/10/21	191.42	228.80	37.38	37.06	1.29	38.59	-	0.03	-
24/11/21	186.62	268.23	81.61	66.13	1.03	82.82	-	0.00	-
23/12/21	346.28	431.23	84.95	40.00	1.31	86.16	-	0.00	-
24/01/22	210.97	251.38	40.41	39.75	0.85	41.62	-	0.03	-
23/02/22	198.83	225.93	27.10	29.11	1.01	28.32	-	0.09	-
23/03/22	242.39	260.00	17.61	52.08	0.85	18.88	-	0.26	-
22/04/22	205.14	226.23	21.09	21.00	1.59	22.33	-	0.17	-
24/05/22	184.65	208.55	23.90	23.03	0.87	25.13	-	0.12	-
22/06/22	274.51	316.97	42.46	44.10	0.80	43.67	-	0.02	-
25/07/22	351.42	411.59	60.17	63.08	0.62	61.38	-	0.00	-
23/08/22	550.56	650.00	99.44	95.78	2.41	100.65	-	0.00	-
22/09/22	365.61	475.87	110.26	100.00	1.13	111.47	116.61	0.00	3.73
24/10/22	243.44	435.33	191.89	180.00	1.55	193.10	196.66	0.00	1.30
23/11/22	276.98	442.50	165.52	178.60	1.33	166.73	170.47	0.00	1.68
15/12/22	327.07	416.87	89.80	91.54	1.38	91.01	97.58	0.00	5.51
24/01/23	131.50	152.12	20.62	19.56	1.16	21.86	42.94	0.18	21.72
23/02/23	129.61	146.76	17.15	15.11	0.93	18.42	40.78	0.28	23.13
23/03/23	106.52	115.64	9.12	8.98	1.55	10.77	36.04	0.97	26.65
25/04/23	97.62	99.17	1.55	4.65	2.12	4.93	31.91	3.24	30.32
23/05/23	83.65	80.17	-3.48	2.61	5.49	2.43	29.35	6.21	32.93
23/06/23	95.07	96.96	1.89	3.59	3.67	5.14	32.09	3.09	30.14
25/07/23	89.44	81.77	-7.67	2.77	9.15	1.23	27.33	9.50	35.22

Table 9: Performance of trading strategy calculated with model for data set 1

JAO Auction	Realised Spread		JAO Price		Model 1		Trading Strategy	
Month	DE→FR	FR→DE	DE→FR	FR→DE	DE→FR	FR→DE	DE→FR	FR→DE
Oct 21	33.55	0.67	18.27	1.08	20.44	0.21	15.28	not exec
Nov 21	41.58	0.67	37.06	1.29	38.59	0.03	4.52	not exec
Dec 21	53.99	0.37	66.13	1.03	82.82	0.00	-12.14	not exec
Jan 22	43.87	0.17	40.00	1.31	86.16	0.00	3.87	not exec
Feb 22	56.75	0.01	39.75	0.85	41.62	0.03	17.00	not exec
Mar 22	43.69	0.49	29.11	1.01	28.32	0.09	not exec	not exec
Apr 22	67.50	0.13	52.08	0.85	18.88	0.26	not exec	not exec
May 22	20.12	0.17	21.00	1.59	22.33	0.17	-0.88	not exec
Jun 22	31.06	0.69	23.03	0.87	25.13	0.12	8.03	not exec
Jul 22	85.90	0.04	44.10	0.80	43.67	0.02	not exec	not exec
Aug 22	28.46	1.16	63.08	0.62	61.38	0.00	not exec	not exec
Sep 22	49.14	0.55	95.78	2.41	100.65	0.00	-46.64	not exec
Oct 22	28.22	2.02	100.00	1.13	111.47	0.00	-71.78	not exec
Nov 22	19.15	0.90	180.00	1.55	193.10	0.00	-160.85	not exec
Dec 22	20.07	0.80	178.60	1.33	166.73	0.00	not exec	not exec
Jan 23	14.64	0.37	91.54	1.38	91.01	0.00	not exec	not exec
Feb 23	20.61	0.16	19.56	1.16	21.86	0.18	1.05	not exec
Mar 23	10.38	0.94	15.11	0.93	18.42	0.28	-4.73	not exec
Apr 23	6.20	0.58	8.98	1.55	10.77	0.97	-2.78	not exec
May 23	2.57	6.74	4.65	2.12	4.93	3.24	-2.08	4.62
Jun 23	1.18	4.64	2.61	5.49	2.43	6.21	not exec	-0.85
Jul 23	5.18	5.14	3.59	3.67	5.14	3.09	1.59	not exec
Aug 23	4.40	7.85	2.77	9.15	1.23	9.50	not exec	-1.30

Table 10: Performance of trading strategy calculated with model for data set 2

JAO Auction	Realised Spread		JAO Price		Model 2		Trading Strategy	
Month	DE→FR	FR→DE	DE→FR	FR→DE	DE→FR	FR→DE	DE→FR	FR→DE
Oct 22	28.22	2.02	100.00	1.13	116.61	3.73	-71.78	0.89
Nov 22	19.15	0.90	180.00	1.55	196.66	1.30	-160.85	not exec
Dec 22	20.07	0.80	178.60	1.33	170.47	1.68	not exec	-0.53
Jan 23	14.64	0.37	91.54	1.38	97.58	5.51	-76.90	-1.01
Feb 23	20.61	0.16	19.56	1.16	42.94	21.72	1.05	-1.00
Mar 23	10.38	0.94	15.11	0.93	40.78	23.13	-4.73	0.01
Apr 23	6.20	0.58	8.98	1.55	36.04	26.65	-2.78	-0.97
May 23	2.57	6.74	4.65	2.12	31.91	30.32	-2.08	4.62
Jun 23	1.18	4.64	2.61	5.49	29.35	32.93	-1.43	-0.85
Jul 23	5.18	5.14	3.59	3.67	32.09	30.14	1.59	1.47
Aug 23	4.40	7.85	2.77	9.15	27.33	35.22	1.63	-1.30

6 Conclusion

Auctions of transmission rights between neighbouring countries are becoming increasingly active. In a parallel development, the introduction of market coupling frequently leads to smaller price differences between such countries. Indeed, if two countries are completely coupled, the price of a given hour of electricity will be identical in each country, resulting in a price spread of zero.

Clearly, it is important to take this market coupling into account when evaluating transmission rights, as neglecting it would lead to a significant overvaluation of this right. In order to address this issue, we introduce a general regime-switching mechanism that can be applied to many models in the literature. We describe the model estimation procedure in detail, and compare model and market prices of European spread options. We observe a dramatic paradigm shift in our data set at the end of the summer of 2021, and show that this shift has a strong effect on the model parameters. We also see that the reliable pricing and trading of spread options has become more problematic.

In future work, it would be interesting to investigate the causes of regime-switching, and introduce the possibility of correlating the states of the regime-switching Markov process to electricity price levels or to other variables. These variables could include market volatility, prices in related markets such as natural gas markets and weather conditions such as sun and wind, which affect the electricity produced by renewable sources.

References

Martin T. Barlow. A diffusion model for electricity prices. Mathematical Finance, 12(4):287–298, October 2002.

Markus Burger, Bernhard Graeber, and Gero Schindlmayr. Managing Energy Risk: An Integrated View on Power and Other Energy Markets. Wiley Finance. Wiley, second edition, 2014.

René Carmona and Valdo Durrleman. Pricing and hedging spread options. SIAM Review, 45(4):627–685, 2003.

Peter Carr and Dilip B. Madan. Option valuation using the Fast Fourier Transform. Journal of Computational Finance, 2(4):61–73, 1999.

Álvaro Cartea and Carlos González-Pedraz. How much should we pay for interconnecting electricity markets? A real options approach. Energy Economics, 34(1):14–30, January 2012.

Álvaro Cartea and Pablo Villaplana. Spot price modeling and the valuation of electricity forward contracts: The role of demand and capacity. Journal of Banking and Finance, 32(12):2502–2519, December 2008.

Álvaro Cartea, Sebastian Jaimungal, and Zhen Qin. Speculative trading of electricity contracts in interconnected locations. Energy Economics, 79:3–20, March 2019.

Troels Sønderby Christensen and Fred Espen Benth. Modelling the joint behaviour of electricity prices in interconnected markets. Quantitative Finance, 20(9):1441–1456, 2020.

Iain J. Clark. Commodity Option Pricing: A Practitioner's Guide. Wiley Finance. Wiley, 2014.

Michael Coulon and Sam Howison. Stochastic behavior of the electricity bid stack: From fundamental drivers to power prices. The Journal of Energy Markets, 2(1):29–69, Spring 2009.

EEX. European Energy Exchange, 2022. https://www.eex.com.

ENTSO-E. European network of transmission system operators for electricity, 2022. https://www.entsoe.eu.

EPEX-SPOT. European Power Exchange, 2022. https://www.epexspot.com.

European Commission Expert Group. Towards a sustainable and integrated Europe. Technical report, European Commission, November 2017. First Report of the Commission Expert Group on Electricity Interconnection Targets, 40 pages.

European Commission Expert Group. Electricity interconnections with neighbouring countries. Technical report, European Commission, November 2018. Second Report of the Commission Expert Group on Electricity Interconnection Targets, 40 pages.

European Commission Expert Group. Contribution of the electricity sector to smart sector integration. Technical report, European Commission, October 2020. Fourth Report of the Commission Expert Group on Electricity Interconnection Targets, 44 pages.

Viviana Fanelli. Financial Modelling in Commodity Markets. Financial Mathematics Series. Chapman and Hall/CRC, first edition, 2019.

Roland Füss, Steffen Mahringer, and Marcel Prokopczuk. Electricity derivatives pricing with forward-looking information. Journal of Economic Dynamics and Control, 58:34–57, September 2015.

Roland Füss, Steffen Mahringer, Florentina Parashiv, and Marcel Prokopczuk. Electricity spot and derivatives pricing under market coupling. Technical report, University of St. Gallen, July 2017. Working Papers on Finance No.2013/23, 53 pages.

Wieger J. Hinderks, Ralf Korn, and Andreas Wagner. A structural Heath–Jarrow–Morton framework for consistent intraday spot and futures electricity prices. Quantitative Finance, 20(3):347–357, March 2020.

JAO. Joint allocation office, 2022. https://www.jao.eu.

Nektaria V. Karakatsani and Derek W. Bunn. Intra-day and regime-switching dynamics in electricity price formation. Energy Economics, 30(4):1776–1797, July 2008.

Rüdiger Kiesel and Michael Kustermann. Structural models for coupled electricity markets. Journal of Commodity Markets, 3(1):16–38, September 2016.

Rüdiger Kiesel and Florentina Paraschiv. Econometric analysis of 15-minute intraday electricity prices. Energy Economics, 64:77–90, May 2017.

Rüdiger Kiesel, Gero Schindlmayr, and Reik H. Börger. A two-factor model for the electricity forward market. Quantitative Finance, 9(3):279–287, April 2009.

Roger W. Lee. Option pricing by transform methods: Extensions, unification, and error control. Journal of Computational Finance, 7(3):51–86, 2004.

Julio J. Lucia and Eduardo S. Schwartz. Electricity prices and power derivatives: Evidence from the Nordic power exchange. Review of Derivatives Research, 5(1):5–50, 2002.

Lucia Parisio and Bruno Bosco. Electricity prices and cross-border trade: Volume and strategy effects. Energy Economics, 30(4):1760–1775, 2008.

Lucia Parisio and Matteo Pelagatti. Market coupling between electricity markets: Theory and empirical evidence for the Italian-Slovenian interconnection. Economia Politica, 36:527–548, 2019.

Elisabetta Pellini. Measuring the impact of market coupling on the Italian electricity market. Energy Policy, 48:322–333, 2012.

Anca Pircalabu and Fred Espen Benth. A regime-switching copula approach to modeling day-ahead prices in coupled electricity markets. Energy Economics, 68:283–302, 2017.

Andrea Roncoroni, Gianluca Fusai, and Mark Cummins. Handbook of Multi-Commodity Markets and Products: Structuring, Trading and Risk Management. Wiley Finance Series. Wiley, 2015.

Simon Elias Schrader and Fred Espen Benth. A stochastic study of carbon emission reduction from electrification and interconnecting cable utilisation. the Norway and Germany case. Energy Economics, 2022.

Eduardo S. Schwartz and Lenos Trigeorgis, editors. Real Options and Investment under Uncertainty: Classical Readings and Recent Contributions. MIT Press, 2001.

Daniel W. Stroock. An Introduction to Markov Processes. Graduate Texts in Mathematics. Springer, 2005.

Lenos Trigeorgis. Real Options Managerial Flexibility and Strategy in Resource Allocation. MIT Press, 1996.

A The Call Option Formula via the Fourier Transform

The characteristic function $\phi = \phi_T$ of the spot price S_T at time T is given for $u \in \mathbb{R}$ by:

$$\phi_T(u) = E[e^{iuS_T}] = \int_{-\infty}^{\infty} e^{iuS} p(S) dS, \tag{26}$$

where p is the probability density function of S_T.

For example, for the Bachelier model:

$$dS_t = \mu dt + \sigma dB_t, \quad S_0 \in \mathbb{R},$$

with drift $\mu \in \mathbb{R}$ and volatility $\sigma > 0$, and with solution:

$$S_T = S_0 + \mu T + \sigma B_T, \quad B_T \sim N(0, T),$$

the characteristic function ϕ^B is given by:

$$\phi^B(u) = e^{iu(S_0+\mu T) - \frac{1}{2}u^2\sigma^2 T}.$$

In general, for a European call option with strike K and maturity T, we have:

$$C(K) = e^{-rT} \int_K^{\infty} (S - K) p(S) dS.$$

For $\alpha > 0$, define the *modified* or *damped call price* by:

$$c(K) = e^{\alpha K} C(K). \tag{27}$$

Then the Fourier transform $\hat{c}$ of c can be calculated as:

$$\begin{aligned}\hat{c}(u) &= \int_{-\infty}^{\infty} e^{iuK} \int_{K}^{\infty} e^{\alpha K}(S-K)p(S)dSdK \\ &= \int_{-\infty}^{\infty} p(S) \int_{-\infty}^{S} (S-K)e^{(\alpha+iu)K}dKdS.\end{aligned}$$

The inner integral is calculated using integration by parts as:

$$\begin{aligned}\int_{-\infty}^{S}(S-K)e^{(\alpha+iu)K}dK &= \underbrace{\left[(S-K)\frac{1}{\alpha+iu}e^{(\alpha+iu)K}\right]_{-\infty}^{S}}_{=0} - \int_{-\infty}^{S} -\frac{1}{\alpha+iu}e^{(\alpha+iu)K}dK \\ &= \left[\frac{1}{(\alpha+iu)^2}e^{(\alpha+iu)K}\right]_{-\infty}^{S} \\ &= \frac{1}{(\alpha+iu)^2}e^{(\alpha+iu)S}.\end{aligned}$$

Using this result, we finally obtain:

$$\begin{aligned}\hat{c}(u) &= \int_{-\infty}^{\infty} p(S)\frac{1}{(\alpha+iu)^2}e^{i(u-i\alpha)S}dS \\ &= \frac{1}{(\alpha+iu)^2}\int_{-\infty}^{\infty} p(S)e^{i(u-i\alpha)S}dS \\ &= \frac{1}{(\alpha+iu)^2}\phi(u-i\alpha).\end{aligned} \tag{28}$$

The call option price is then obtained via Fourier inversion as:

$$C(K) = \frac{e^{-\alpha K}}{2\pi}\int_{-\infty}^{\infty} e^{-iuK}\hat{c}(u)du. \tag{29}$$

Since the imaginary part of the integrand is odd in u, and the real part even, this integral can also be calculated as:

$$C(K) = \frac{e^{-\alpha K}}{\pi}\int_{0}^{\infty} \Re\left[e^{-iuK}\hat{c}(u)\right]du. \tag{30}$$

Note that the function $\hat{c}$ has a pole of order 2 at $u = i\alpha$.

An equivalent formulation is often found in the literature, e.g., Lee (2004) and Cartea and González-Pedraz (2012), which we will present next. By introducing the variable $z = u - i\alpha$, and using $iz = iu + \alpha$, we can define the function $\hat{C}$ as:

$$\begin{aligned}\hat{c}(u) &= \int_{-\infty}^{\infty} p(S)\frac{1}{(\alpha+iu)^2}e^{i(u-i\alpha)S}dS \\ &= -\int_{-\infty}^{\infty} p(S)\frac{1}{z^2}e^{izS}dS \\ &= -\frac{1}{z^2}\phi(z) \\ &=: \hat{C}(z).\end{aligned}$$

In terms of the transform $\hat{C}$, the call option price is expressed as:

$$\begin{aligned} C(K) &= \frac{e^{-\alpha K}}{2\pi}\int_{-\infty}^{\infty} e^{-iuK}\hat{c}(u)du \\ &= \frac{e^{-\alpha K}}{2\pi}\int_{-\infty-i\alpha}^{\infty-i\alpha} e^{-i(z+i\alpha)K}\hat{C}(z)dz \\ &= \frac{1}{2\pi}\int_{-\infty-i\alpha}^{\infty-i\alpha} e^{-izK}\hat{C}(z)dz \\ &= -\frac{1}{2\pi}\int_{-\infty-i\alpha}^{\infty-i\alpha} e^{-izK}\frac{1}{z^2}\phi(z)dz \end{aligned}$$

We denote the integrand above as a function g,

$$g(z) := e^{-izK}\frac{1}{z^2}\phi(z),$$

and proceed to calculate the residue of g at $z = 0$, or $u = i\alpha$ in terms of the variable u. Using (26) together with the exponential series, we can expand g as:

$$\begin{aligned} g(z) &= \int_{-\infty}^{\infty}(1 + izS + ...)(1 - izK + ...)\frac{1}{z^2}p(S)dS \\ &= \int_{-\infty}^{\infty}(1 + izS - izK + ...)\frac{1}{z^2}p(S)dS \\ &= \int_{-\infty}^{\infty}(\frac{iS}{z} - \frac{iK}{z} + ...)p(S)dS. \end{aligned}$$

Since

$$\frac{d}{du}\phi(u) = \phi'(u) = E[iSe^{iuS}] = \int_{-\infty}^{\infty} iSe^{iuS}p(S)dS,$$

it follows that the residue has two components R_1 and R_2, with:

$$\begin{aligned} R_1 &= \int_{-\infty}^{\infty} iSp(S)dS = \phi'(0) = iE[S_T], \\ R_2 &= \int_{-\infty}^{\infty} -iKp(S)dS = -iK\phi(0) = -iK, \end{aligned}$$

and we obtain:

$$R = R_1 + R_2 = i(E[S_T] - K). \tag{31}$$

Finally,

$$-\frac{1}{2\pi}\oint g(z)dz = -\frac{1}{2\pi}\cdot 2\pi i R = E[S_T] - K.$$

Our main contributions are:
1) We increase the resolution from daily (peak, off-peak) electricity prices to hourly prices, and add regime-switching to reflect coupled and decoupled hours.
2) We perform a simulation exercise to demonstrate that our regime-switching model successfully captures the important stylised features of intermittently connected markets.
3) We show that our model can adapt to the new market paradigm of high prices, uncertainty and volatility.
4) We find that the pricing of spread options works well in a ``normal'' market environment. However, in a highly volatile environment, both auction and model ex ante spread option prices may turn out to lie far from ex post realised payoffs.